Dynamic Demand Modeling Incorporating Renewable Energy Sources Using a Population-Based Optimization Method

LUIS CARLOS PÉREZ GUZMÁN[1], GINA MARÍA IDÁRRAGA OSPINA[1],
FREDDY BOLAÑOS MARTÍNEZ[2], SERGIO RAÚL RIVERA RODRÍGUEZ[3]

[1]Facultad de Ingeniería Mecánica y Eléctrica,
Universidad Autónoma de Nuevo León
San Nicolás de los Garza, Nuevo León,
MEXICO

[2]Departamento de Energía Eléctrica y Automática,
Universidad Nacional de Colombia SEDE Medellín,
COLOMBIA

[3]Departamento de Ingeniería Eléctrica,
Universidad Nacional de Colombia SEDE Bogotá,
COLOMBIA

Abstract: - Due to the inclusion of distributed generation (DG) in microgrids (MGs), the accelerated growth in demand, and environmental concerns, suitable management and operational strategies are imperative. The utilization of wind and solar energy has rapidly increased in MGs. However, due to the uncertainties these systems present, accurately predicting energy generation remains challenging. This necessitates modeling the system's random variables (such as renewable resource output and possibly load demand) using appropriate and feasible methods. The primary objective of this article is to determine the optimal setpoints for renewable energy sources (RES) and all elements involved in the MG, minimizing the total operation cost. The system comprises wind turbines (WT), photovoltaic panels (PV), energy storage systems (ESS), and electric vehicles (EVs). Weibull distribution and the Hottel and Liu Jordan equations are employed to determine the potential available capacity of wind and solar energy generation, respectively. ESS is utilized to enhance MG performance. For optimal management, a comprehensive mathematical model with practical constraints for each MG element is extracted. An efficient Population-Based Incremental Learning (PBIL) metaheuristic method is proposed to solve the optimization objective in an MG, demonstrating that this energy management system optimizes and effectively coordinates DG and ESS energy generation considering economic considerations. Finally, PBIL is compared with a commonly used model, Particle Swarm Optimization (PSO), across various scenarios, analyzing and evaluating their outcomes, showcasing a reduction in operation costs.

Key-Words: - optimization, microgrid, uncertainty, cost, algorithm, particle swarm optimization, energy management, Weibull, solar photovoltaic, wind.

1 Introduction

The utilization of distributed generation (DG) technologies to address continuous improvement, efficiency, and reliability within the electrical system, coupled with the competition in the electricity market and the reduction of greenhouse gases, represents a relatively new market being adopted by both users and power-generating companies. DGs encompass renewable units such as wind turbines (WT), photovoltaic panels (PV), or biomass, alongside non-renewable units like fuel cells, microturbines, gas engines, diesel generators, etc. DGs eliminate the need for the transmission system by being installed close to the demand. The integration and control of DGs with storage devices and flexible loads can form a low-voltage distribution network, termed a microgrid (MG), capable of operating in isolated mode or interconnected with the main distribution grid as an entity. This implies functioning either for self-consumption or facilitating energy import/export to/from the MG, [1], [2], [3], [4], [5], [6].

Today, the implementation of the MR concept, due to its low operational costs within the system and environmental aspects, is expanding across the distribution network. From the perspective of MR owners, economic operation is crucial. Given that MRs can participate in energy markets and provide ancillary services, appropriate scheduling becomes essential. Therefore, a suitable strategy for MR operation must be pursued, [2].

MRs often face difficulties meeting total demand due to energy shortages, as the energy generated by DG sources is sometimes insufficient. This challenge arises from the intermittent nature of certain renewable energy (RE) resources, necessitating an energy management system to address this issue. Energy management systems for a microgrid represent relatively new and popular topics that have recently garnered significant attention.

One of the main challenges in managing certain renewable resources like wind and solar energies is the issue of uncertainty in their behavior. That is, the actual energy production from these resources differs from the forecasted values in real time. This can be defined as the probability of the difference between the predicted and actual values. In other words, owing to the uncertainty in energy production from these resources, the operator's responsibility is to maintain a balance between production and consumption, which poses certain challenges. Therefore, system operators attempt to provide a certain amount of reserve energy through the energy storage system (ESS) to cover uncertainty in energy production and maintain system security at the desired level, [3].

MR users can indeed overcome this shortage by purchasing more energy from the utility company or by increasing the number of generating sources. However, these solutions often come with higher emission and energy costs, referring to either purchasing from the grid or the cost of the elements involved. Another solution to mitigate this problem and maintain a balance between system production and consumption is by reducing customer consumption during periods of energy scarcity. This practice of demand competing with offers made by production units is termed 'Demand Response' (DR). DR is defined as changes in end-user electrical usage in their normal consumption patterns in response to changes in electricity prices over time or incentives designed to induce lower electricity usage during high wholesale market prices or when system reliability is compromised, [3].

To optimize MR operation, different objective functions have been considered, as in [2], [3], [4], along with the utilization of various types of RE sources. One such source is wind energy, which has emerged as a significant RE alternative. However, due to its fluctuations, various methods have been considered for energy generation forecasting for optimal scheduling of WT, [5]. In [2] and [6], a probabilistic method for wind speed prediction based on recorded values was proposed. This model, called 'Weibull Distribution,' is used to model stochastic variables and has been employed by various authors for short-term wind speed prediction. Consequently, WT output power can be estimated based on the technical constraints specified by the manufacturer.

Both wind and solar energy encounter challenges regarding fluctuation in power production. References as [7], [8], [9], [10], [11], address this issue based on certain established equations. For proper system functioning, configuring the optimal amount of purchased energy before system operation initiation is crucial. This is because without knowledge of the available PV power on an operational day, determining the exact quantity required from the grid becomes difficult. Photovoltaic energy is estimated by calculating solar energy radiation, using the modified Hottel equation and the Liu-Jordan equation. These equations also address the issue of partially cloudy/rainy weather, determining the site-specific climate for photovoltaic production. The authors in [12] and [13], analyzed the values behind these equations, such as solar constants, solar hours, declination, and zenith angle, among other data, to achieve the desired outcome. Therefore, to estimate photovoltaic output power, the method described in [14], [15], [16], [17], [18], [19], has been utilized, comprising a set of technical formulas supported by technical data specified by the PV manufacturer. Regarding the previously mentioned ESS in [3], the focus was on the State of Charge (SOC) limits for its proper operation within the MG.

Currently, there is a growing trend towards the use and adoption of electric vehicles (EVs) due to fossil fuel depletion and increasing environmental concerns. Adopting electric vehicles as an alternative mode of transportation necessitates the development of a charging infrastructure. The behavior of the EV battery (BEV) in its SOC closely correlates with the ESS. Despite varying EV handling, displacement can be defined through a pattern, supported by the SOC, to predict the amount of stored energy due to such EV displacement, [20], [21], [22].

Optimization involves handling variations using information from an initial concept to improve it. Many engineering industry problems, especially in manufacturing systems, are inherently complex and challenging to solve using conventional optimization techniques, [23]. Finally, an efficient metaheuristic method, Population-Based Incremental Learning (PBIL), is proposed to resolve the conflicting objective problem (cost and coordination) for optimal operation, employing a simple algorithm that utilizes a probability vector to generate the population, considering the highest evaluations of the vector, [24] and [25]. To evaluate the proposed algorithm, the management system is applied to a typical MR consisting of multiple ER generators, ESS, EVs, and electrical loads. The results showcase effective coordination of GD and ESS energy generation considering economic and environmental considerations.

Many researchers have employed the Particle Swarm Optimization (PSO) algorithm for improvement purposes. The PSO algorithm is typically utilized to minimize the operational cost of distributed energy resources while considering network constraints, demand response, and the incorporation of renewable resources in electrical studies. Previous studies have not precisely addressed the uncertainties caused by wind turbines and solar panels from the demand side. Favorable results were obtained compared to the Probabilistic Binary Particle Swarm Optimization (PBIL) method. This study employs a programming model to minimize the total operating costs in a Microgrid (MR), encompassing energy generation with stochastic behavior of Wind Turbines (WT) and Photovoltaic (PV) panels along with associated uncertainties. Additionally, since implementing a real open electricity market is not feasible in many existing distribution and energy systems due to underdeveloped communication infrastructure, this paper interacts with demand bids for each element used to address this issue and create a competitive energy market. The analysis facilitates the operator's decision-making by observing the power behaviors and costs of all energies to be incorporated into the main system. This decision-making can assist the operator in anticipating whether certain energy sources can be practically utilized, minimizing risks or maximizing benefits, whether in terms of energy or economics. A multi-objective system considering the cost analysis of uncertainty due to the integration of renewable sources into the main system is a future-oriented approach related to the optimization of this work's system. A comparison between the PSO and PBIL methods is presented in the final section of the document, due to the greater use of PSO in such problems, noting some similarities in the methods. However, there is a certain error percentage in favor of the proposed method, reducing the estimated cost.

2 System to Model

In this section, the proposed stochastic model in the MG, shown in Figure 1, encompasses Renewable Energy Sources (RES) and user load demands. Additionally, random interruptions in DGs, variability in both the SOC of ESS and EV batteries (BEVs) and the grid market are modeled. The framework of the considered MG relies on planning units to supply demand optimally and suitably through wind and solar energy generation elements, primarily through natural stochastic behavior. The inclusion of EVs is an innovation that will likely become commonplace shortly, hence its fundamental incorporation. Energy is supplied within 24 hours by energy generation consisting of utility services, WT, PVs, and ESSs for EVs and user loads. Therefore, energy production calculation relies on operations with certain restrictions or limits.
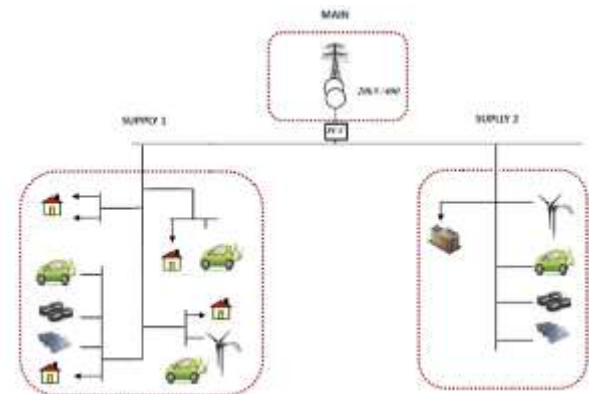

Fig. 1: Proposed Microgrid

The forecasted amount of wind speed, solar irradiance, and load is generated through established and commonly used methods today, [7], [8], [9], [10], [11], supported by long-term historical data, although the latter was acquired through daily routine activities. All these values, considered as input values at the system's outset, represent the average forecasted amount produced per hour in the day. Finally, the MG generates multiple scenarios involving possible stochastic quantities, aiming to optimize minimum operational costs in residential loads while considering specific constraints for each device to address uncertainties caused by wind and solar energy generation.

2.1 Photovoltaic System Modeling

A simplified schematic of the developed system is depicted in Figure 2. The maximum nominal output of the PV or photovoltaic system used in the proposed system is 275W per module. The ESS consists of sufficient capacitor modules to meet demand, with each unit's maximum capacity set at 300 watts. To simulate different hourly load patterns throughout the day, an estimate of the usage for various electrical appliances commonly found in households today was applied, resulting in variable loads ranging from a minimum of 50W to a maximum of 1150W.

The system's output power is determined by user-provided data, in addition to the values from the following sections. This article focuses on the northern region of Mexico, specifically in Monterrey, Nuevo León. The city is located at latitude 25°40' North and longitude 100°18'West, at an elevation of 537 meters above sea level, with a Peak Solar Hour (PSH) of 5.2 and temperatures around 30 degrees Celsius.
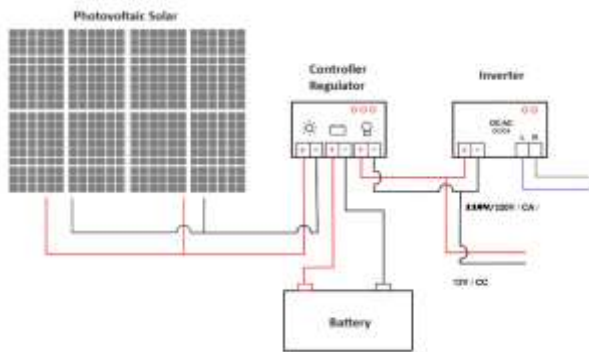

Fig. 2: Photovoltaic system

2.1.1 Hottel's y Liu Jordan Equations

The references in [7], [8], [9], [10], [11], the Hottel method allows for estimating global radiation under clear atmospheric conditions based on the location's latitude, altitude, and climate characteristics, categorized into four types as shown the Table 1, [12]. This model expresses atmospheric transmittance for direct radiation, τ_b, as a function of the zenith angle, θ_z.

Table 1. Climate characteristics

Climate Type	r_O	r_1	r_K
Tropical	0.95	0.98	1.02
Summer, mid-latitude	0.97	0.99	1.02
Summer, sub-artic	0.99	0.99	1.01
Winter, mid-latitude	1.03	1.01	1.00

The daily output power of the PV has been estimated by calculating daily solar radiation. The calculation of beam radiation τ_b utilized the modified Hottel equation shown in Equation 1

$$\tau_b = \alpha_0 + \alpha_1 + e^{\frac{K}{\cos(\theta_z)}} \tag{1}$$

where a_0, a_1, and k are parameters depending on the altitude above sea level A in the geographical area under analysis (0.1736, 0.7097, and 0.3493, respectively). The zenith angle is represented by $\cos(\theta_z)$. Subsequently, the modified Liu Jordan equation is used to find diffuse radiation τ_d in Equation 2.

$$\tau_d = 0.2710 - 0.2939(\tau_d) \tag{2}$$

The solar constant G_{cs} is used to obtain values in W/m2, as in [12], [13].

$$G_{on} = G_{cs} * \left(1 + \left(1 + 0.033 * \cos\frac{360n}{365}\right)\right) \tag{3}$$

Using equations 1, 2, and 3, the value of total solar radiation is obtained. The Figure 3 show the values of irradiance.
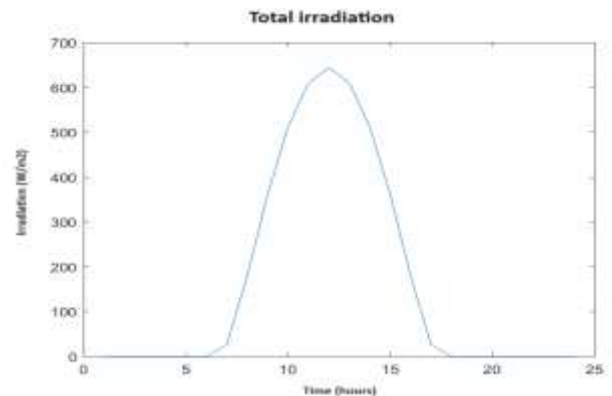
$$G_t = G_{on} * (\tau_b + \tau_d) \tag{4}$$

Fig. 3: Total solar irradiation on January 1st, 2020

2.1.2 Solar Panel Power

The output power P_{pv} of the photovoltaic module depends on solar energy, irradiance, ambient temperature of the location, and the characteristics of the module itself.

$$T_m = T_a + G_t\left(\frac{NOCT - 20}{G_t NOCT}\right) \tag{5}$$

$$I_m = I_{sc} * \left(\frac{G_t}{G_t NOCT} + \left(1 + \left(\frac{T_{I_{sc}}}{100}\right) * (T_m - 25)\right)\right) \tag{6}$$

$$V_m = V_{oc} - \left(\frac{T_{V_{oc}}}{100}\right) * (T_m - 25) \tag{7}$$

$$FF = \frac{V_{mp} + I_{mp}}{V_{oc} + I_{sc}} \tag{8}$$

$$P_{pv}(t) = FF * V_m * I_m * NM \tag{9}$$

Where the values of Table 2 are provided by the manufacturer:

Table 2. Characteristics of the manufacturer

T_m = Module temperature in degrees Celsius °C.
T_a = Ambient temperature in degrees Celsius °C.
G_t = Total Irradiation (W/m2) at time t.
G_tNOCT = Normal Operation Cell Temperature (800 W/m2).
G_tSTC = Standard Test Condition (1000 W/m2).
I_m = Current at maximum power in Amps.
I_{sc} = Module short-circuit current in Amps.
V_m = Voltage at maximum power in volts.
V_{oc} = Module open-circuit voltage in volts.
T_{Isc} = Current temperature coefficient in °C.
T_{Voc} = Voltage temperature coefficient in °C.
NM = Number of solar modules
FF = Fill Factor.

The Figure 4 shows the power behavior in watts due to the production of energy by the photovoltaic system.

2.2 Wind System Modeling

In this document, the concept of reliable capacity is used to model uncertainty, representing the availability of wind energy. The power fluctuation caused by wind speed variation is not extremely random in terms of magnitude and ramp speeds.
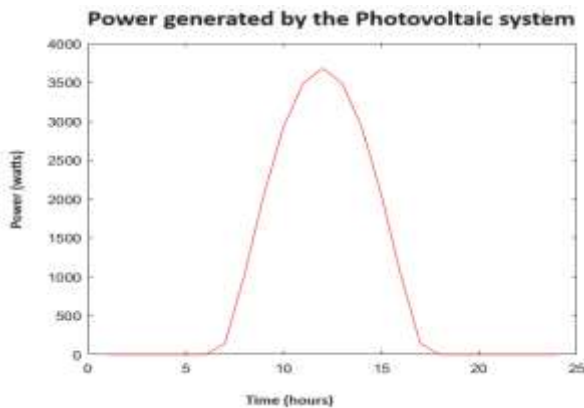
Fig. 4: Estimated power of the modules on January 1st, 2020

The output of wind power will be based on the uncertainty presented by the wind speed in a region. The probability of wind speed occurrence, i.e., the frequency of each wind speed, is analytically expressed by the Weibull distribution, [3].

The power curve is the most feasible method for annual production use and is much more accurate. For the study, an AW-1500/70 wind turbine model from the manufacturer Acciona was used (Table 3).

Table 3. Technical characteristics of the AW 1500/70 wind turbine

Parameter	Unit
Manufacturer	Acciona (Spain)
Power	1500 watts
Diameter	70 m
Swept area	3849 m^2
Power density	2.57 m^2/kW
Number of blades	3

The energy produced by a wind turbine is the result of adding all the products of the powers (Pi) delivered in each time interval (t) by the duration of each interval in hours during a given period (day, month, year, depending on the desired calculation). Therefore, the energy E is expressed in a simplified manner as shown in Equation 10.

$$E = \sum P_i * \Delta t \tag{10}$$

Where P_i is the power at each time interval in watts, and Δt is the duration of each time interval in hours.

This approach allows for a comprehensive understanding of wind energy generation over a specified period.

2.2.1 Weibull Distribution

To handle the uncertainty in wind energy generation due to wind speed, a statistical probability method like the Weibull Distribution is employed for a given time frame. Data is collected over a month, comprising 24-hour intervals, in a region where the installation of these wind turbines is planned. An anemometer captures these data points, as displayed in Figure 5, obtained from [24]:
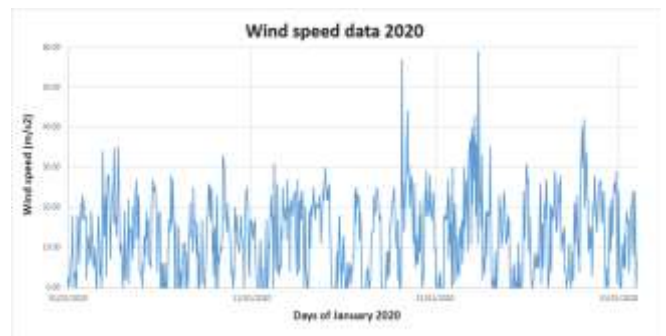
Fig. 5: Recorded wind speed data

When wind speed measurements are taken annually, the Weibull probability distribution function successfully describes frequency curves, [26]. The Weibull probability density function is expressed as:

$$f(v) = \frac{k}{c} * \left(\frac{v}{c}\right)^{k-1} * e^{-\left(\frac{v}{c}\right)^k} \tag{11}$$

here, k is the shape parameter, and c is the scale parameter. The equation 11 provides the probability that the wind speed falls within a 1 m/s interval centered at that speed. To fit the frequency data to the Weibull function, the values of parameters k and c will be determined via a non-linear fitting process, show in Figure 6. This process aims to find suitable values for these parameters based on the wind speed data illustrated in Figure 5.
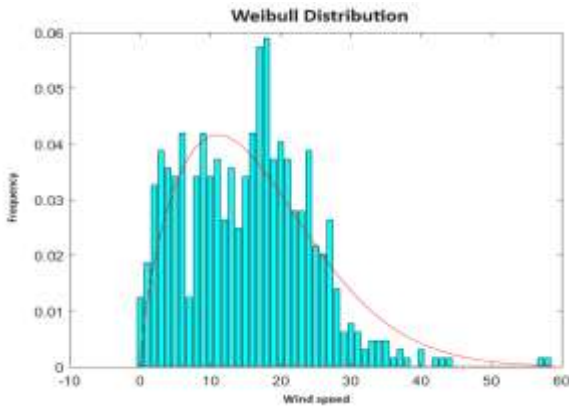

Fig. 6: Fit Weibull graph

2.2.2 Average Wind Power

The turbine power is independent of the Weibull function; that is, analyzing wind speed at a location helps calculate the average velocity. The Weibull distribution accurately determines the probability of a specific wind speed occurring. When wind data is modeled using $f(v)$, the average wind power (P_v) perpendicular to an area (A) is given by Equation 12 [26]:

$$P_v = 0.5 A\rho \int_0^\infty v^3 f(v)\, dv \tag{12}$$

It can be shown that when $f(v)$ is the Weibull distribution function, the average power delivered is given by Equation 13:

$$P_v = \frac{A\rho v^3 \Gamma\left(1 + \frac{3}{k}\right)}{2\left[\Gamma\left(1 + \frac{1}{k}\right)\right]^3} \tag{13}$$

The power output constraints of a wind turbine utilized in this study are illustrated below:

$$P_v = \begin{cases} 0 & v < v_{in} \text{ and } v > v_{out} \\ p_{wr}\left(\dfrac{v - v_{in}}{v_r - v_{in}}\right) & v_{in} <= v <= v_r \\ p_{wr} & v_r < v <= v_{out} \end{cases} \tag{14}$$

Here, v_{in} and v_r represent the cut-in and rated wind speeds of the turbine (m/s), respectively, while v_{out} signifies cut-out of wind velocity.

2.3 Energy Storage System Modeling

The Energy Storage System (ESS) consists of electrochemical batteries electrically connected to an energy source and the load, playing a vital role in managing an Interconnected Microgrid (IM). To optimize the operational planning of an IM, a suitable mathematical model for the ESS has been developed in [3], [5], [6].

As per Equation 15, the battery's charging and discharging rates in each one-hour interval over the operational period should stay within predetermined limits, as defined in Equation 16.

The charge and discharge rate of the battery in each one-hour interval of the entire operation period must be within an estimated limit.

$$|P_{charge,t}| \leq P_c^{max}$$
$$|P_{discharge,t}| \leq P_{dis}^{max} \tag{15}$$

The state of charge (SOC) must not violate the default maximum and minimum value.

$$SOC_{min} \leq SOC(t) \leq SOC_{min} \dots \forall t \in T \tag{16}$$

The battery is authorized to change its state of charge and discharge only once per operating period within the specified period.

The constraints regarding the power limits that the ESS can charge or discharge within a time t are depicted in Equation 17, considering the efficiency of the charging or discharging process (η_c and η_d), and the current and previous energy states (SOC_{Sj} (t) and SOC_{Sj} (t-1)).

$$SOC_{Sj}(t) = SOC_{Sj}(t-1) + \eta c \sum_{t=1}^{T} P_{SCj}(t) - \frac{1}{\eta d}\sum_{t=1}^{T} P_{SDj}(t) \tag{17}$$
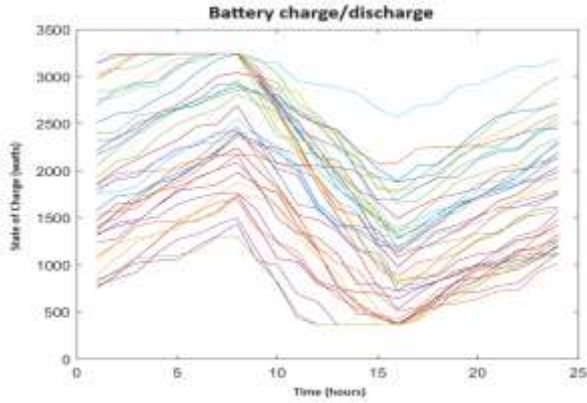
Fig. 7: ESS battery charge/discharge

Figure 7 illustrates the behavior exhibited by the battery within the energy storage system over the course of the day. Typically, following manufacturer recommendations, the battery is designed with a certain tolerance in its design to prevent wear on its components, establishing a limit on its charge/discharge to preserve its lifespan. The energy storage system regulates the power output of the system in case of any disturbances in the Microgrid (MG), among other functions. Primarily, in this analysis, its usage is to supply residential, commercial, or industrial sectors in cases where the production from renewable sources is insufficient to meet the expected demand. Alternatively, depending on operational costs or market conditions, energy may be utilized as an auxiliary means for other areas of the system through exchange, benefiting both the prosumer and the main system. The troughs in the graph represent the maximum energy at that moment within the Energy Storage System (ESS) (not necessarily reaching 100% to preserve its lifespan), while the peaks represent the discharge of the ESS (not necessarily 0%), either due to usage within the area. Each area's behavior depends on various factors, primarily revolving around the sale and purchase of energy from the grid. In this study, random values were chosen to represent batteries with different initial capacities to visualize their charge/discharge behavior throughout the day, interacting with other sources that need to meet the user's demand.

2.4 Electric Vehicle Modeling

The modeling of Electric Vehicle (EV) charging is highly stochastic due to the need to consider the driving patterns of EV users, in [20], [21], [22]. Parameters such as arrival time, departure time, distance covered by an EV user, charging rate, etc., are necessary to model EV demand. In this study, it is assumed that from 6 AM to 7 PM, the EV is disconnected from the Microgrid (MG), resulting in

a certain percentage of power loss. Upon returning home at the specified time, the Battery Electric Vehicle (BEV) reconnects to charge overnight, and the State of Charge (SOC) of the EV evolves in an independent random pattern.

The energy consumed due to the vehicle's daily distance is determined by the Equation 18:

$$SOC_d = \left(1 - (dist/dt)\right) \qquad (18)$$

Here, SOC_d represents the energy consumption due to the distance traveled by the EV in a day (*dist*) concerning the total range (dt) it can cover. The initial SOCE of the BEV during charging is calculated using Equation 19:

$$SOC_E = SOC_E(t-1) - SOC_E(t) \\ * \left(1 - (dist/dt)\right) \qquad (19)$$

Where *dist* and *dt* denote the traveled distance and the maximum range of the EV, respectively. Charging stops from 7 AM onwards. The algorithm saves the last state of charge, so when the EV returns home at 8 PM, the discharge ratio based on the distance covered from the last state determines the SOC_E of the EV.

Figure 8 depicts the electric vehicle battery behavior throughout the day. The scenario is utilized solely for the study in this article, where in the BEV does not exchange energy with the main grid, and the stored energy is utilized when renewable sources do not entirely meet the user's demand. However, for future endeavors, the intention is to explore energy exchange with the grid.
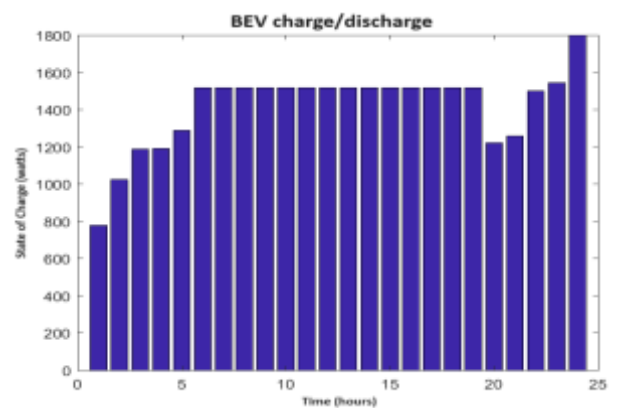

Fig. 8: Battery EV charge/discharge

3 Microgrid Configuration

3.1 Cost Minimization Function

The operational cost function comprises cost summation functions for each production unit (DGs), energy reserve costs (ESS and EV), and utility exchange (grid), [3].

$$Min_{f(x)} = \sum_{d=1}^{D}\sum_{d=1}^{D} CT_{DG}(t) + CT_{S}(t) + CT_{EV}(t) + CT_{G}(t) \qquad (20)$$

Each cost summation interval involves the costs of the involved DG sources (CT_{GD}) in the Microgrid (Equation 21), the energy storage system costs represented by CT_{S} in Equation 22, and the EV costs by CT_{EV} E in Equation 23. Finally, the grid cost is denoted as CT_{G} in Equation 24. Each equation specifies its bid (B) in the market as well as the power (P) being produced by the source at that moment, considering if it's active ON/OFF (U).

$$CT_{DG}(t) = \sum_{i=1}^{N_{DG}} U_{i}(t) * P_{DG_{i}}(t) * B_{DG_{i}}(t) \qquad (21)$$

$$CT_{S}(t) = \sum_{j=1}^{N_{S}} U_{j}(t) * P_{S_{j}}(t) * B_{S_{j}}(t) \qquad (22)$$

$$CT_{EV}(t) = \sum_{e=1}^{N_{EV}} U_{e}(t) * P_{EV_{e}}(t) * B_{EV_{e}}(t) \qquad (23)$$

$$CT_{G}(t) = U_{G}(t) * P_{G}(t) * B_{G}(t) \qquad (24)$$

The flowchart in Figure 9 displays the algorithm used by the program when evaluating the objective function, where different systems within the Microgrid interact concerning time t. It demonstrates decision-making regarding the time t for the SOC_{S} of the energy storage system battery and the SOC_{E} of the electric vehicle, along with the generated power to meet the demanded load. The ultimate result is the total cost of the energies used at that moment.
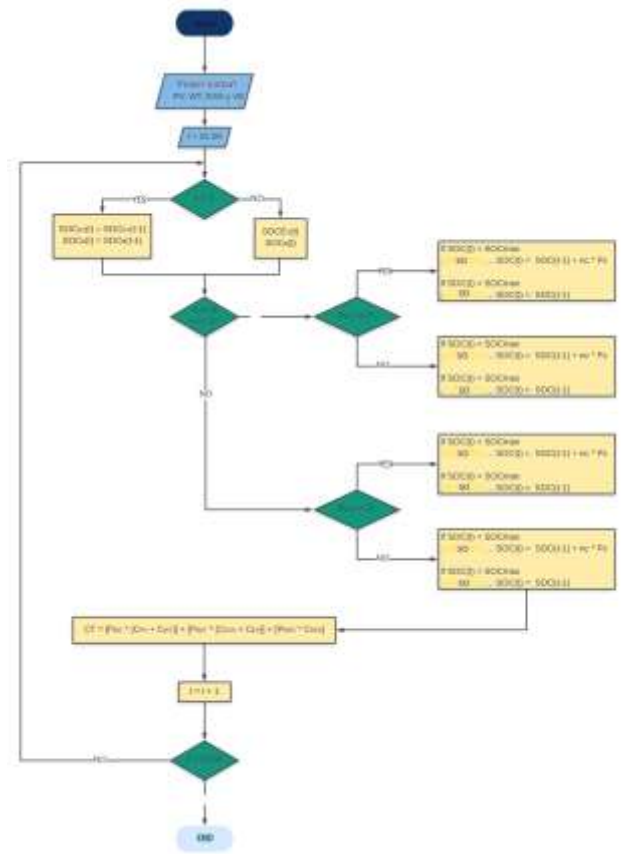

Fig. 9: Objective function evaluation.

3.2 Energy Balance Constraints

The total generated power in each interval must equal the total load demands, the energy stored in the battery bank (charge/discharge), electric vehicles (charge/discharge), and total feeder losses (Eq.25):

$$\sum_{i=1}^{N_{DG}} P_{DG_{i}}(t) + \sum_{j=1}^{N_{S}} P_{S_{j}}(t) + \sum_{e=1}^{N_{EV}} P_{EV_{e}}(t) + P_{G}(t) = P_{L}(t) \qquad (25)$$

This equation considers each energy source used to meet the user's demand, where P_{GD} is the sum of all power sources i of DG (wind and solar), P_{S} is the energy stored by batteries j at time t, P_{EV} is the energy of BEVs e at time t, P_{G} is the energy delivered by the main grid to the consumer due to the ER sources not entirely meeting the user's demand, and finally P_{L} is the total electrical load demand at time t.

3.3 Power Variable Constraints

3.3.1 Distributed Generation Powers

The powers generated by the DG sources establish limits on their values, as shown in Equation 26.

$$P_{DG_{min}} \leq P_{DG}(t) \leq P_{DG_{max}} \qquad (26)$$

where $P_{DG_{min}}$ (t) y $P_{DG_{max}}$ (t) are the minimum and

maximum active power of distributed generation at time t, respectively.

$$0 \leq P_{PV}(t) \leq P_{PV_{kwp}} \tag{27}$$

$$0 \leq P_{WT}(t) \leq P_{WT_{max}} \tag{28}$$

3.3.2 ESS and BEV Battery

Both the State of Charge (SOC) and the charge/discharge power (P_{SC}/P_{SD}) have their respective limits established during the analysis. In practice, completely discharging a battery reduces its lifespan, so the battery should maintain a minimum energy capacity, and ideally, a maximum capacity 29. Charging/discharging powers must also adhere to the manufacturer's specifications 30.

$$SOC_{min} \leq SOC(t) \leq SOC_{max} \tag{29}$$

$$P_{S_{min}} \leq P_S(t) \leq P_{S_{max}} \tag{30}$$

These values also apply to the electric vehicle's battery, where, based on manufacturer data, the SOC and charge/discharge powers, considering their efficiency (η), play a significant role.

$$\frac{1}{\eta_D} \sum_{t=1}^{T} P_{EV_j}(t) + \eta_C \sum_{t=1}^{T} P_{EV_j}(t) \tag{31}$$

Although the equations for the energy storage battery and the electric vehicle's battery are similar, it all depends on the distance and times at which the electric vehicle connects to the grid.

4 Method for Microgrid Optimization and Case Studies

4.1 Population-Based Incremental Learning (PBIL) Algorithm

Optimally managing energy in an MR involves solving a combination of problems using metaheuristic methods. The Population-Based Incremental Learning (PBIL) algorithm has been employed for its suitable capabilities in handling such issues. The authors in [23], [24], [25], mention that PBIL is an evolutionary algorithm that works by updating a vector describing univariate statistics of the best solutions. This straightforward model update is controlled by a parameter that sets the Learning Ratio (LR). The model is then used to generate new solutions. The optimal energy management procedure is illustrated in the Figure 10.

```
function PBIL(pot.random, bounds)
    BinaryX ← initialize_population
    while I<Iterations Time do
        DecimalX ← BINARY TO DECIMAL
        NomX ← NORMALIZE POWER
        #evaluar ← COST FUNCTION
        if cost < cost(t - 1) then
            return {cost}        ▷ stores the best value
        end if
        selection ← THE BEST VALUES 50%
        if selection = 1 then
            return {sel + 1}      ▷ increases probability
        end if
        Update ← PROBABILITY VALUES
        if I > 1 then
            return {P_I * (1 - LR) + BinaryX_max * LR}
        end if
        Generate ← NEW POPULATION BINARYX
        I = I + 1
    end while
    return BEST INDIVIDUAL
end function
```

Fig. 10: Pseudocode PBIL

The algorithm iteratively updates the probability values of the Vector Probability (VP), starting from neutral values. Each iteration or generation creates a population of individuals based on the current VP probabilities. The best individuals from a given generation update the VP values for the next generation. Algorithm execution stops when the VP converges, i.e., when all elements become zero or one, or when the specified iteration count is reached, [23].

The VP update follows the equation:

$$VP = VP * (1 - LR) + BinaryX_{max} * LR \tag{32}$$

Where VP is the vector probability, LR is the learning ratio and the variable *BinaryX_max* is the best individual in binary form.

Updating the VP considers the Learning Ratio (LR), a crucial factor in implementation that determines the speed and accuracy of obtaining results. In essence, LR is the important factor given to the best individual for VP update.

4.2 Simulation and Results

The Microgrid (MG) depicted in Figure 1, connected to the electric grid, was analyzed as the test system in this document. The system's maximum demand is represented by the total energy of all loads contributing to the main system, akin to a typical household.

Hence, the daily load curve for the MG is showcased in Figure 11. The total energy consumption for the day equaled 42320 kWh. Constraints and data for the involved sources are presented in Table 4.
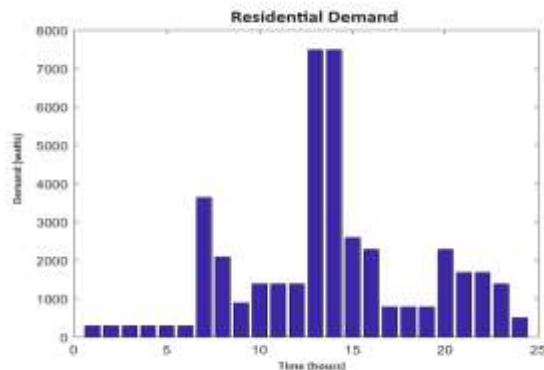

Fig. 11: Daily demand curve for a residence

Table 4. Limits of the Sources Involved.

Units	Minimum power (watts)	Maximum power (watts)
PV	0	8250
WT	0	1500
ESS	-330	250
EV	-500	400

The system integrates various technologies like WT, PS, ESS and EV, assuming real-time hourly market prices presented in Table 5. The output power of WT and PV systems is illustrated in Table 6 based on predicted values. Distributed Generation (DG) systems are strategically placed in different branches to encompass diverse or hybrid systems.

4.2.1 Case Studies

Scenarios 1 and 2 consider the operational costs of all units alongside problem constraints. Scenario 1 aims to minimize operational costs, integrating GDs at their maximum power. Scenario 2 involves all GDs using random power capacities. Scenarios 3 and 4 focus on a single distributed energy source. Scenario 3 incorporates random power from PS with its storage system, while Scenario 4 employs WT power as the sole source.

Table 5. Market price, Hourly rates

Time	PV	WT	ESS	Grid
1	0	0.0210	0.1192	0.033
2	0	0.0170	0.1192	0.027
3	0	0.0125	0.1269	0.020
4	0	0.0110	0.1346	0.017
5	0	0.0510	0.1423	0.017
6	0	0.0850	0.1500	0.029
7	0	0.0910	0.1577	0.033
8	0.0646	0.1100	0.1608	0.054
9	0.0654	0.1400	0.1662	0.215
10	0.0662	0.1430	0.1677	0.572
11	0.0669	0.1500	0.1731	0.572
12	0.0677	0.1550	0.1769	0.572
13	0.0662	0.1370	0.1692	0.215
14	0.0654	0.1350	0.1600	0.572
15	0.0646	0.1320	0.1538	0.286
16	0.0638	0.1140	0.1500	0.279
17	0.0653	0.1100	0.1523	0.086
18	0.0662	0.9250	0.1500	0.059
19	0	0.0910	0.1462	0.050
20	0	0.0830	0.1462	0.061
21	0	0.0330	0.1431	0.181
22	0	0.0250	0.1385	0.077
23	0	0.0210	0.1346	0.043
24	0	0.0170	0.1269	0.037

Table 6. Predicted values for WT and PV

Time	WT (watts)	PV (watts)	Time	WT (watts)	PV (watts)
1	249.5	0	13	17.5	5931.9
2	399.0	0	14	60.7	5120.9
3	519.5	0	15	140.3	3866.7
4	727.1	0	16	252.0	2362.2
5	503.8	0	17	496.0	1095.6
6	324.3	0	18	611.4	0
7	138.6	1094.4	19	412.7	0
8	87.7	2361.8	20	327.3	0
9	89.0	3866.2	21	183.3	0
10	17.5	5120.0	22	133.6	0
11	6.4	5931.4	23	96.7	0
12	8.1	6211.2	24	138.6	0

The management of ESS entails specific schedules for charging and discharging towards the MR or the main grid. Charging occurs when energy prices are relatively low, irrespective of user demand. Conversely, during high energy prices, the battery supplies the demanded load. Surplus renewable energy might charge these batteries if the production exceeds user demand.

In all the above scenarios, BEVs are solely considered as loads, not contributing energy to the residence. Their restricted hours were mentioned in Section 2.

4.2.2 Scenario 1 and 2: Comparative Analysis

The outcomes of Scenario 1, outlined in Table 7, reveal the configuration of participating units with their optimal power generation. Notably, the ESS contributes to the MR during high market prices and to the grid during lower price periods. Meanwhile, the BEV acts purely as a load, showing no participation. These power outputs originate from randomly assigned values in the photovoltaic and wind systems.

Table 7. Scenario 1 with random power in WT and PV

Time	PV	WT	ESS	EV	Grid
1	0	250	0	0	1200
2	0	399	0	0	1051
3	0	519	0	0	931
4	0	727	0	0	723
5	0	0	0	0	1450
6	0	0	0	0	1450
7	1094	0	0	0	17106
8	0	0	0	0	10450
9	3866	89	330	0	165
10	5120	17	330	0	1483
11	5931	6	330	0	682
12	6211	8	330	0	401
13	5932	17	330	0	31171
14	5121	61	330	0	31939
15	3867	140	330	0	8613
16	2360	250	327	0	8513
17	1096	0	0	0	2854
18	0	0	0	0	3950
19	0	0	0	0	3950
20	0	0	0	0	11450
21	0	183	0	0	8267
22	0	134	0	0	8316
23	0	97	0	0	6853
24	0	139	0	0	2361

Figure 12 depicts the generated power (red line) versus the power used (blue bars) by the photovoltaic system. On the other hand, Figure 13 illustrates the power generated (red line) by the wind turbine against the power consumed by the user (blue bar) sourced from wind energy.

Scenario 2 (Table 8) showcases the optimal power configuration of renewable sources when operating at maximum capacity. Minimal reliance on the main grid is observed, as it entirely fulfills the demand, leading to a considerable reduction in energy costs.
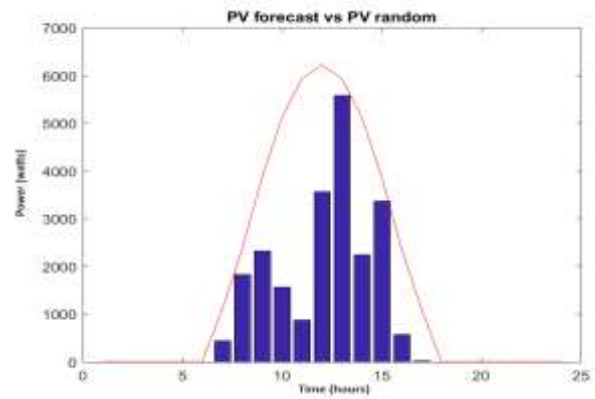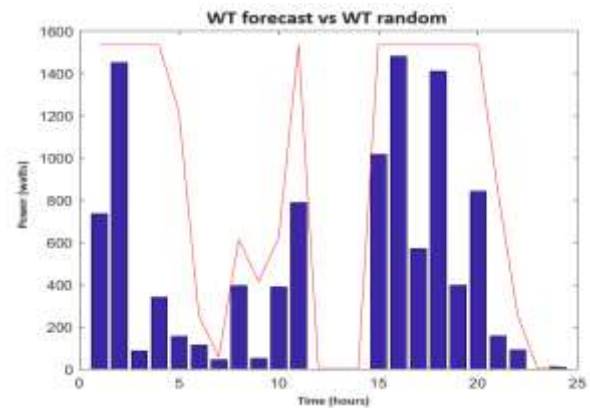

Fig. 12: Random powers PV

Fig. 13: Random powers WT

Table 8. Scenario 1 with maximum power in WT and PV

Time	PV	WT	ESS	EV	Grid
1	0	1450	0	0	0
2	0	1450	0	0	0
3	0	1450	0	0	0
4	0	1450	0	0	0
5	0	1216	0	0	234
6	0	251	0	0	1199
7	1094	57	0	0	17049
8	2362	611	0	0	7477
9	3866	412	330	0	159
10	5120	617	330	0	883
11	5931	1022	-3	0	0
12	6211	0	330	0	409
13	5932	0	330	0	31188
14	5121	0	330	0	31999
15	3867	1533	330	0	7220
16	2362	1533	330	0	7225
17	1096	1533	0	0	1321
18	0	1533	0	0	2417
19	0	1533	0	0	2417
20	0	1533	0	0	9917
21	0	840	0	0	7610
22	0	252	0	0	8198
23	0	0	0	0	6950
24	0	17	0	0	2483

The complete utilization of energy generated by the GD systems is depicted in Figure 14 and Figure 15.
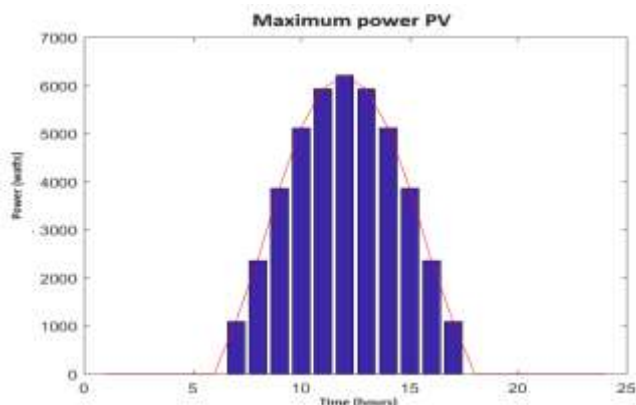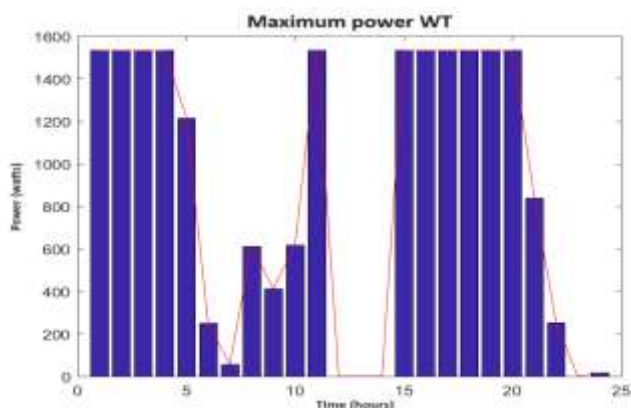

Fig. 14: Maximum powers PV

Fig. 15: Maximum powers WT

4.2.3 Scenario 3 and 4: Comparative Analysis

In Scenario 3, as indicated in Table 9, the energy generation from a DG source, specifically the WT, is crucial. The absence of PV production during the early hours necessitates total reliance on the main grid. However, post-noon, the ESS is compelled to operate at maximum capacity due to substantial power output from the WT.

There's a similarity between Scenario 3 and Scenario 4 due to the absence of a power-generating source. This is evident in Figure 19, where a significant reduction in the optimal cost is observed.

Table 9. Scenario 1 with maximum power in PV

Time	PV	WT	ESS	EV	Grid
1	0	0	0	0	1450
2	0	0	0	0	1450
3	0	0	0	0	1450
4	0	0	0	0	1450
5	0	0	0	0	1450
6	0	0	0	0	1450
7	1094	0	0	0	17106
8	2362	0	0	0	8088
9	3866	0	330	0	254
10	5120	0	330	0	1500
11	5931	0	330	0	689
12	6211	0	330	0	1409
13	5932	0	330	0	31188
14	5121	0	330	0	31999
15	3867	0	330	0	8753
16	2362	0	330	0	8758
17	1096	0	0	0	2854
18	0	0	0	0	3950
19	0	0	0	0	3950
20	0	0	0	0	11450
21	0	0	0	0	8450
22	0	0	0	0	8450
23	0	0	0	0	6950
24	0	0	0	0	2500

4.3 Optimal Cost Analysis

The graph in Figure 16 demonstrates the participation of all involved sources. However, due to minimal energy generation, there was an exchange of energy with the main grid, resulting in the algorithm finding an optimal cost of $950.
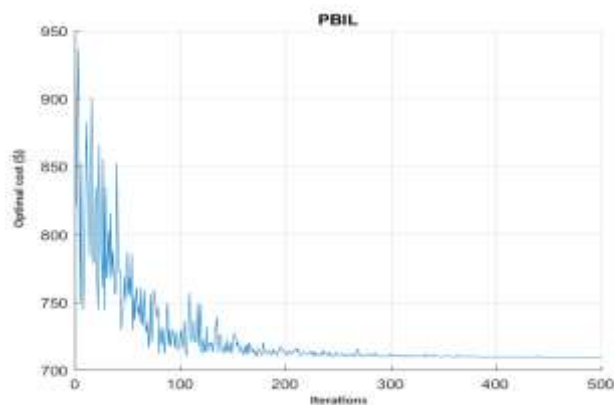

Fig. 16: Optimal cost with random powers in PV and WT

In contrast, the optimal cost for Scenario 2 is depicted in Figure 17, showcasing a notable reduction compared to Scenario 1.
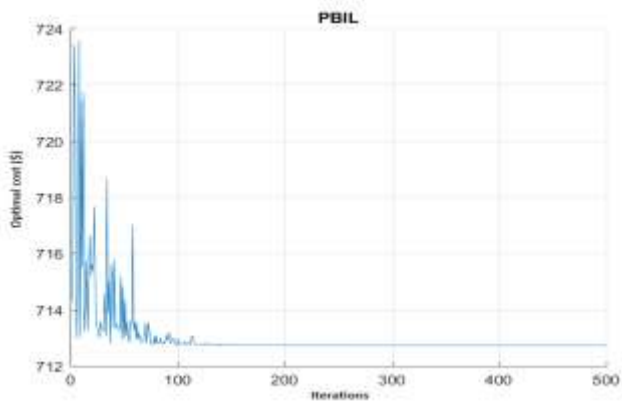
Fig. 17: Optimal cost with maximum powers in PV and WT

The highest cost is exhibited in Scenario 4 in Figure 18, attributed to the null PV production during peak hours when the market price is high. This necessitates additional wind power generation. However, Scenario 3 showcases behaviour where the power configuration is more suitable, resulting in the lowest optimal cost range (Figure 18).
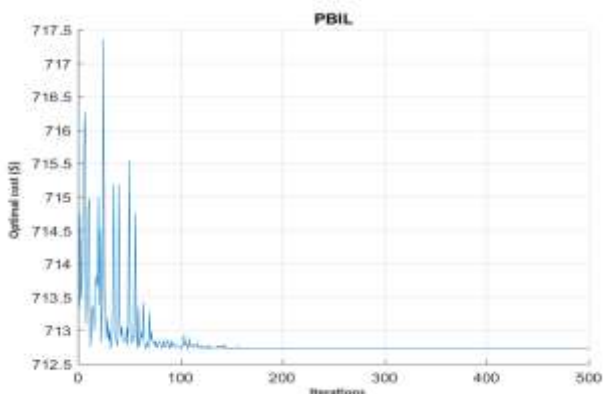
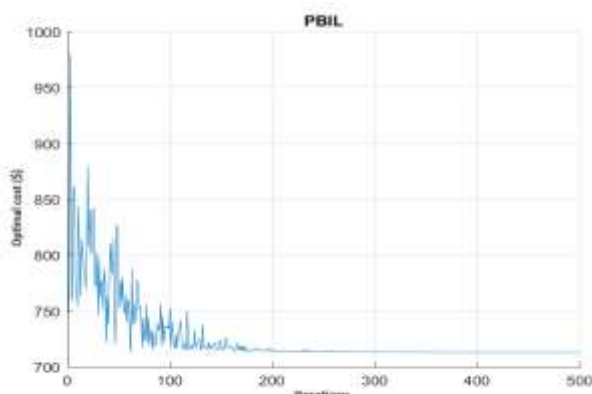

Fig. 18: Optimal cost with maximum power in PV without WT

Fig. 19: Optimal cost with maximum power in WT without PV

4.4 Comparative Analysis. Particle Swarm Optimization

With the aim of juxtaposing the PBIL method against one of the most widely cited metaheuristic approaches in the academic domain, particularly pertinent in addressing optimization challenges involving operational costs, emissions reduction, and optimal power allocation, the Particle Swarm Optimization algorithm (PSO) emerged as the most fitting candidate for this comparative analysis, [6], [7], [9], [13], [14]. Noteworthy for its adeptness in optimal resource management, PSO operates as an intelligent swarm algorithm predicated on the collective movement of particles traversing the solution space. Each constituent entity, or 'particle,' within the PSO framework navigates the search space with a velocity dynamically modulated in response to its own exploration history and that of its neighboring particles.
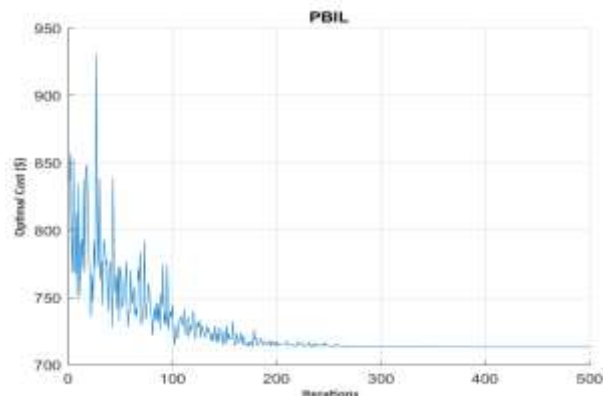

Fig. 20: Optimal cost with random powers in PV and WT using PBIL
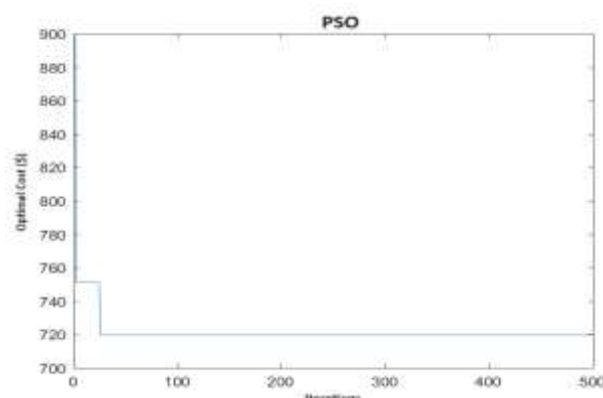

Fig. 21: Optimal cost with random powers in PV and WT using PSO

Figure 20 and Figure 21 show the comparison made between the proposed method PBIL and the most used method for this type of problem, which is PSO. For this study, it was concluded that the

computational response time with the PSO method is slightly slower than the PBIL method, under the same conditions (equal number of iterations). However, PSO converges faster than PBIL. The advantage of PBIL lies in its practicality in modelling, clearly illustrating the behavior of the graphs in the process. The methodology of the applied methods depends on the programmer and variables, limits, and factors such as the population or chromosomes to be selected. It is worth mentioning that the speed of the response goes hand in hand with the objective function that was proposed. Figure 20 and Figure 21 use the maximum power of solar and wind energy.

5 Conclusion

The proposed method for optimizing operating costs and optimal values within a microgrid composed of various renewable energy sources is conducive to such analysis and may offer equal or greater reliability compared to alternative methodologies commonly employed for this purpose. The results obtained across different scenarios provide insights into the behavior of generation systems within the microgrid and their interaction with the main system. The algorithm functions effectively within the proposed scenarios, successfully fulfilling its purpose of providing optimal values that benefit the user in terms of both cost and power. Scenarios 1 and 2 demonstrate a reduction in optimal costs attributable to the management performed by the algorithm in adjusting power levels, a phenomenon evident with each iteration as new populations are generated to find the most suitable solution.

Scenarios 3 and 4, on the other hand, exhibit enhanced responsiveness, with the system converging in approximately half the iterations compared to Scenario 1. It is worth noting that initiating with relatively high or maximum power values leads to decreased iterations and costs, albeit contingent upon how the algorithm optimizes its values to align with the objective function being addressed. This algorithm affords an equal or superior perspective on the step-by-step process of searching for potential solutions aimed at achieving optimal values for efficient system operation.

The outcomes presented in this study underscore how adjustments to operational limits, chromosome and population selection, as well as the learning rate (LR), directly impact the magnitude and swiftness of the results obtained.

References:
[1] H. Shayeghi, E. Shahryari, M. Moradzadeh, P. Siano, A Survey on Microgrid Energy Management Considering Flexible Energy Sources, *Review energies MDPI*, Vol.12, 2019, pp. 2156, doi:10.3390/en12112156.

[2] S. Talari, M. Yazdaninejad, Mahmoud-Reza Haghifam, Stochastic-based scheduling of the microgrid operation including wind turbines, photovoltaic cells, energy storages and responsive loads, *IET Generation, Transmission and Distribution*, Vol.9, No.12, 2015, pp. 1498-1509.

[3] G.R. Aghajani, H.A. Shayanfar, H. Shayeghi, Presenting a multi-objective generation scheduling model for pricing demand response rate in micro-grid energy management, *Elsevier Energy Conversion and Management*, Vol.106, 2015, pp. 308-321.

[4] A. A. Moghaddam, A. Seifi, T. Niknam, M. Reza A. Pahlavani, Multi-objective operation management of a renewable MG (micro-grid) with back-up micro-turbine/fuel cell/battery hybrid power source, *Elsevier Energy*, Vol.36, 2011, pp. 6490-6507.

[5] M. Motevasel, A. R. Seifi, Expert energy management of a micro-grid considering wind energy uncertainty, *Elsevier Energy Conversion and Management*, Vol.86, 2014, pp. 58-72.

[6] S. A. Alavi, A. Ahmadian, M. Aliakbar-Golkar, Optimal probabilistic energy management in a typical microgrid microgrid based-on robust optimization and point estimate method, *Elsevier Energy Conversion and Management*, Vol.95, 2015, pp. 314-325.

[7] C. Chen, S. Duan, T. Cai B., Liu G. Hu, Smart energy management system for optimal microgrid economic operation, *IET Renewable Power Generation*, Vol.5, No.3, 2012, pp 258-267.

[8] Md. H. Rahman, S. Yamashiro, Novel Distributed Power Generating System of PVECaSS Using Solar Energy Estimation, *IEEE Transactions on Energy Conversion*, Vol.22, No.2, 2007, pp. 358-367.

[9] H. Rahman, K. Nakamura, S. Yamashiro, A Study on the Performance of Grid-Connected PV-ECS System Considering Meteorological Variation, *15th PSCC*, Vol.27, 2005, pp. 22-27, Liege, Belgium.

[10] M. H. Rahman, F. Yasmin, Khademul Islam, A Study on the Performance of Grid-Connected PV-ECS System Considering

Meteorological Variation of Bangladesh, Vol.59, No.2, 2011, pp. 249-256.

[11] Md. H. Rahman, K. Nakamura, S. Yamashiro, Development of an Advanced Grid-Connected PV-ECS System considering Solar Energy Estimation. *Kitami Institute of Technology, IEEJ Trans. PE*, Vol.125, No.4, 2005, pp. 399-407.

[12] J. A. Duffie, W. A. Beckman, *Solar Engineering of Thermal Processes*, Wiley, Fourth Edition 2013, ISBN 978-0-470-87366-3.

[13] G. Abal, V. Durañona, *Manual Tecnico de Energia Solar Termica, Volumen I: Fundamentos*, Facultad de Ingeniería, Vol.1, 2013, ISBN 178-9974-0-0910-3.

[14] Y. M. Atwa, El-Saadany, M. M. A. Salama, R. Seethapathy, Optimal Renewable Resources Mix for Distribution System Energy Loss Minimization, *IEEE Transactions on Power Systems*, Vol.25, No.1, 2010, pp. 360-370.

[15] Z. M. Salameh, B. S. Borowy, Atia R. A. Amin, Photovoltaic Module-Site Matching Based on the Capacity Factors, *IEEE Transactions on Energy Conversion*, Vol. 10, No. 2, 1995, pp. 326-332.

[16] Y. Riffonneau, S. Bacha, F. Barruel, S. Ploix, Optimal Power Flow Management for Grid Connected PV Systems with Batteries, *IEEE Transactions on Sustainable Energy*, Vol.2, No.3, 2011, pp. 309-320.

[17] E. Skoplaki, J.A. Palyvos, On the temperature dependence of photovoltaic module electrical performance: A review of efficiency/power correlations, *Elsevier Solar Energy*, Vol.83, 2009, pp. 614–624.

[18] K. Brecl, M. Topic, Photovoltaics (PV) System Energy Forecast on the Basis of the Local Weather Forecast: Problems, Uncertainties and Solutions, energies MDPI, Vol.11, 2018, pp. 1143, doi:doi:10.3390/en11051143.

[19] P. M. Segado, J. Carretero, M. S. Cardona, Models to predict the operating temperature of different photovoltaic modules in outdoor conditions, *Progress in Photovoltaic*, 2014, DOI: 10.1002/pip.2549.

[20] T. Rawat, Khaleequr R. Niazi, N. Gupta, S. Sharma, Impact assessment of electric vehicle charging/discharging strategies on the operation management of grid accessible and remote microgrids, *Shor Communication WILEY Energy Research*, 2019, pp. 1-15, DOI: 10.1002/er.4882.

[21] T. Rawat, K. Rehman Niazi, Comparison of EV smart charging strategies from multiple stakeholders' perception, *The 6th International Conference on Renewable Power Generation The journal Engineering*, Vol. 2017, Vol.13, 2017, pp. 1356–1361, doi: 10.1049/joe.2017.0553.

[22] A. Rabiee, M. Sadeghi, J. Aghaeic, A. Heidari, Optimal operation of microgrids through simultaneous scheduling of electrical vehicles and responsive loads considering wind and PV units uncertainties, *Renewable and Sustainable Energy Reviews*, Vol.57, 2016, pp. 721–739.

[23] Luis A. Cruz Prospero, Manuel Mejía Lavalle, José Ruiz Ascencio, Virna V. Vela Rincón, Population-Based Incremental Learning as Good Alternative for Genetic Algorithms, *Research in Computing Science*, No.116, 2016, pp. 51–64.

[24] Baron, C.; Al-Sumaiti, A.S.; Rivera, S. Impact of Energy Storage Useful Life on Intelligent Microgrid Scheduling. *Energies* 2020, *13*, 957.

[25] Baluja, Population-Based Incremental Learning: A Method for Integrating Genetic Search Based Function Optimization and Competitive Learning, School of Computer Science Carnegie Mellon University, 1994, pp. 3-41.

[26] A. M. Sanchez, G. E. Coria, A. A. Romero and S. R. Rivera, "An Improved Methodology for the Hierarchical Coordination of PEV Charging," in *IEEE Access*, vol. 7, pp. 141754-141765, 2019.

Contribution of Individual Authors to the Creation of a Scientific Article (Ghostwriting Policy)

Conceptualization G.M.I., F.B.M., L.C.P., S.R. ; methodology, , L.C.P.; software, L.C.P and F.B.M.; validation, L.C.P, G.M.I., F.B.M.; formal analysis, , L.C.P, G.M.I.; investigation, L.C.P., G.M.I.; resources, , L.C.P, G.M.I., data curation, L.C.P and F.B.M.; writing—original draft preparation, L.C.P. , S.R.; writing—review and editing, L.C.P, G.M.I., F.B.M.; visualization, , L.C.P.; supervision, G.M.I., F.B.M.; project administration, , G.M.I. , S.R.. The authors have read and agreed to the published version of the manuscript.

Conflict of Interest

The authors have no conflicts of interest to declare.